THE JOURNAL OF BIOLOGICAL CHEMISTRY VOL. 288, NO. 2, pp. 1079–1087, January 11, 2013

Blocking c-Jun N-terminal Kinase (JNK) Translocation to the Mitochondria Prevents 6-Hydroxydopamine-induced Toxicity *in Vitro* and *in Vivo*[*] [S]

Received for publication, September 20, 2012, and in revised form, November 5, 2012 Published, JBC Papers in Press, November 26, 2012, DOI 10.1074/jbc.M112.421354

Jeremy W. Chambers[1], **Shannon Howard, and Philip V. LoGrasso**[2]

From the Department of Molecular Therapeutics and Translational Research Institute, The Scripps Research Institute, Jupiter, Florida 33458

Background: Little is known about the role for JNK mitochondrial signaling in neuronal cell death.
Results: Global and mitochondrial inhibition of JNK protects against 6-OHDA-induced neuronal loss in the SNpc.
Conclusion: Blocking JNK mitochondrial translocation or JNK inhibition may be an effective treatment for neuronal death in Parkinson disease.
Significance: These findings suggest a new molecular target for JNK inhibition.

Because oxidative stress and mitochondrial dysfunction are well known contributors to Parkinson disease (PD), we set out to investigate the role mitochondrial JNK plays in the etiology of 6-hydroxydopamine-induced (6-OHDA) oxidative stress, mitochondrial dysfunction, and neurotoxicity in SHSY5Y cells and neuroprotection and motor behavioral protection *in vivo*. To do this, we utilized a cell-permeable peptide of the outer mitochondrial membrane protein, Sab (SH3BP5), as an inhibitor of JNK mitochondrial translocation. *In vitro* studies showed that 6-OHDA induced JNK translocation to the mitochondria and that inhibition of mitochondrial JNK signaling by Tat-Sab$_{KIM1}$ protected against 6-OHDA-induced oxidative stress, mitochondrial dysfunction, and neurotoxicity. Administration of Tat-Sab$_{KIM1}$ via an intracerebral injection into the mid-forebrain bundle increased the number of tyrosine hydroxylase immunoreactive neurons in the substantia nigra pars compacta by 2-fold ($p < 0.05$) in animals lesioned with 6-OHDA, compared with animals treated only with 6-OHDA into the nigrostriatal pathway. In addition, Tat-Sab$_{KIM1}$ decreased the D-amphetamine-induced unilateral rotations associated with the lesion by 30% ($p < 0.05$). Steady-state brain levels of Tat-Sab$_{KIM1}$ at day 7 were 750 nM, which was ~3.4-fold higher than the IC$_{50}$ for this peptide *versus* Sab protein. Collectively, these data suggest that 6-OHDA induced JNK translocation to the mitochondria and that blocking this translocation reduced oxidative stress, mitochondrial dysfunction, and neurotoxicity both *in vitro* and *in vivo*. Moreover, the data suggest that inhibitors that block association of JNKs with the mitochondria may be useful neuroprotective agents for the treatment of Parkinson disease.

The role of mitochondrial JNK is emerging as a significant new area of study, and the resulting oxidative stress, mitochondrial dysfunction, and cell death caused by this translocation have been associated with numerous cell types, tissues, and disease states (1–6). Oxidative stress and mitochondrial dysfunction are hallmarks of PD[3] (7–9), and understanding the mechanisms and therapeutic strategies to reduce these abnormalities could prove clinically beneficial. Additionally, a significant body of literature implicates JNK as an attractive therapeutic target for preventing neurodegeneration and providing behavioral benefits in genetic and animal models of PD (10–13). Hence, understanding the role of mitochondrial JNK in PD models could prove very valuable.

Wiltshire *et al.* (14) established the outer mitochondrial membrane protein Sab (SH3BP5) as the JNK-interacting binding partner for JNK mitochondrial association. Analysis of Sab indicated it had a kinase-interacting motif (KIM domain) similar to that of many other known JNK-interacting proteins (15–18). The JNK-interacting protein-1 is most well studied, and a cell-permeable version of this peptide has been shown to be efficacious in numerous efficacy models ranging from PD (13) to cerebral ischemia (19) and diabetes (20). Recently, we designed a retro-inverso peptide containing the HIV-Tat sequence along with 20 residues from the Sab KIM1 domain (Tat-Sab$_{KIM1}$), which could also be used for *in vivo* purposes (21). Utilizing both JNK and Sab siRNA silencing, along with peptide mimicry with Tat-Sab$_{KIM1}$, we demonstrated that prevention of JNK translocation to the mitochondria was protective against reactive oxygen species (ROS) generation, dissipation of the mitochondrial membrane potential, and cytotoxicity induced by anisomycin in HeLa cells, and this occurred in a nucleus-independent fashion. Indeed, this peptide has been shown to be highly selective for the JNK pathway over the p38

* This work was supported, in whole or in part, by National Institutes of Health Grant U01NS057153-04 (to P. L.). This work was also supported by The Saul and Theresa Esman Foundation. Philip LoGrasso serves as a consultant for OPKO Health.
[S] This article contains supplemental Fig. 1.
[1] Present address: Department of Cellular Biology and Pharmacology, Herbert Wertheim College of Medicine, Florida International University, Miami, FL 33199.
[2] To whom correspondence should be addressed. Tel.: 561-228-2230; Fax: 561-228-3081; E-mail: lograsso@scripps.edu.

[3] The abbreviations used are: PD, Parkinson disease; 6-OHDA, 6-hydroxydopamine; SNpc, substantia nigra pars compacta; TH, tyrosine hydroxylase; ANOVA, analysis of variance; ROS, reactive oxygen species; OCR, oxygen consumption rate; TAMRA, 6-carboxy-*N*,*N*,*N*′,*N*′-tetramethylrhodamine; LPO, lipid peroxide; ML, mediolateral; DV, dorsoventral; AP, anterior-posterior.

pathway (6, 21). These results, coupled with our demonstration that highly selective JNK inhibitors, such as SR-3306 that do not inhibit p38, PI3K, Akt, and over 300 other kinases (10), are efficacious in protecting dopaminergic neurons and providing behavioral benefit in 6-OHDA-lesioned rats (11), led us to hypothesize that Tat-Sab_{KIM1} could provide the same benefits in neuronal cells and in rats.

This study was designed to test if blocking JNK translocation to the mitochondria would prevent 6-OHDA-induced neurotoxicity. To do this, we utilized SHSY5Y cells and the 6-OHDA lesion model in rats and monitored ROS generation, mitochondrial membrane potential, oxygen consumption rate (OCR), protein carbonylation, lipid peroxidation *in vitro*, and neuroprotection of dopaminergic neurons and behavioral improvement *in vivo*. The major findings showed that 6-OHDA induced JNK translocation to the mitochondria, and blocking this translocation with Tat-Sab_{KIM1} peptide reduced ROS generation, protein carbonylation, and lipid peroxidation, and it increased mitochondrial membrane potential and OCR *in vitro*, while increasing the number of TH^+ neurons and decreasing the D-amphetamine-induced circling *in vivo*.

EXPERIMENTAL PROCEDURES

Cell Culture and 6-OHDA Treatment—Human SHSY5Y cells (ATCC) were grown in DMEM/F-12 (1:1) media supplemented with 10% fetal bovine serum, penicillin, and streptomycin as per the manufacturer's instructions. SHSY5Y cells were used for studies between passages 5 and 17. SHSY5Y cells were passaged using AccuMax cell counting solution to transfer cells among tissue culture vessels. Rat primary cortical neurons were purchased from Invitrogen and grown according to the product insert. Cells were treated with 25 μM 6-OHDA solubilized in dimethyl sulfoxide (DMSO). For measurements involving ROS generation, 6-OHDA was solubilized in *N*,*N*-dimethylformamide to prevent DMSO-induced ROS generation. Cells were incubated in 6-OHDA for 4 h for JNK-related Western blots and mitochondrial translocation studies. Mitochondrial dysfunction measures were taken at either 12, 18, or 24 h as indicated below. Cell viability was monitored at 24 h post-6-OHDA treatment.

Western Blot Analysis—2.5×10^5 SHSY5Y cells were seeded into a 6-well plate and then treated as described in the individual experiments. In the case of monitoring JNK signaling, cell lysates were harvested and then resolved by SDS-PAGE. Proteins were transferred to PVDF membranes using an iBlot apparatus (Invitrogen). Membranes were blocked a minimum of 1 h at room temperature and then incubated with primary antibodies for a minimum of 2.5 h. Most antibodies were purchased from Cell Signaling Technologies, with the exception of the Sab antibody, which was purchased from Novus Biomedical. Membranes were washed and then incubated with DyLight antibodies (680 and 800) purchased from Cell Signaling Technologies for 1 h. Western blots were developed using the Li-Cor Biosciences Odyssey near-infrared scanner. Fluorescent quantitation of Western blots was performed using the software accompanying the Odyssey scanner. Normalized fluorescence was determined based on the ratio of the band of interest to a loading control for individual treatments and divided by the ratio for untreated cells.

Mitochondrial Isolation—Purification of mitochondria was conducted according to the protocol described in our previous research (6, 21). Briefly, 2.5×10^8 SHSY5Y cells were grown on 150-mm^2 tissue culture plates as described above. The cells were washed twice in room temperature PBS, and the cells were scraped gently from the culture surface. Cells were pelleted by centrifugation at $1000 \times g$ for 15 min at room temperature. The pellet was resuspended at six times the pellet volume with ice-cold cell homogenization buffer (150 mM $MgCl_2$, 10 mM KCl, 10 mM Tris-HCl, pH 6.7), and the suspension was placed on ice for 2 min. Using an ice-cold homogenizer, the cells were disrupted with up to 10 up-and-down strokes (disruption was confirmed by microscopy). To the disrupted cells, cell homogenization buffer with 0.25 M sucrose was added at one-third the volume of the suspension followed by gentle inversion to mix thoroughly. The nuclei were pelleted by centrifugation at $1000 \times g$ for 5 min at 4 °C. The supernatant was centrifuged at $5000 \times g$ for 10 min at 4 °C. The pellet was resuspended in ice-cold sucrose/Mg^{2+} buffer (150 mM $MgCl_2$, 250 mM sucrose, 10 mM Tris-HCl, pH 6.7). The pellet was disrupted with an ice-cold Dounce homogenizer with a few strokes. The solution suspension was centrifuged at $5000 \times g$ for 10 min at 4 °C. To remove endoplasmic reticulum membranes from the mitochondria, the mitochondrial pellet was centrifuged through a Histodenz/Percoll gradient. Mitochondria found in the pellet were resuspended in the indicated buffers for the following experiments. The purity of the mitochondrial enrichments was determined using Western blot analysis for mitochondrial resident protein, cytochrome oxidase, cytosolic protein, enolase, nuclear contamination with histone-H3, and microsomal constituent calnexin. Mitochondria were diluted to a concentration of 80 mg/ml, then frozen on dry-ice/ethanol slurry, and stored at −80 °C until use.

Gene Silencing—Knockdown of JNK and Sab was conducted as described in our previous publications (6, 21). Briefly, SHSY5Y cells were grown to 60% confluency in the apparatus required for specific assays. Cells were transfected with siRNAs using the Qiagen Hiperfect reagent according to the supplier's instructions. siRNAs for JNK and controls were purchased from Cell Signaling Technologies, and Sab-specific siRNAs were purchased from Novus Biomedical.

Cell Viability—Cell viability was monitored by TUNEL assay (Millipore) and Cell Titer-Glo (Promega) assay as described in our previous works (6, 21). For these 96-well plate assays, 4×10^4 cells were seeded in a 96-well plate and then treated as described in the experiments. TUNEL and Cell Titer Glo assays were conducted in accordance with the manufacturer's protocol.

Mitochondrial Dysfunction—ROS generation, oxygen consumption, ATP production, and mitochondrial membrane potential were monitored as described in our previous research (6, 21). Using 96-well plate formats, 4×10^4 cells were seeded and then monitored for ROS generation using MitoSOX Red (Invitrogen), oxygen consumption on the Seahorse Biosciences XF-96 extracellular flux analyzer, ATP production by the ATP determination kit protocol (Invitrogen), and mitochondrial membrane potential via JC-1 staining (Cayman Chemical). The

results for ROS, oxygen consumption, and ATP production were measured at 12 h post-stress, whereas mitochondrial membrane potential was measured at 18 h post-stress.

Oxidative Stress Measurements—As described above for the measurements of mitochondrial dysfunction, oxidative stress was measured in a 96-well plate format with 4×10^4 cells per well. Measurement of reduced glutathione was performed using the Glutathione-Glo assay kit from Promega according to the manufacturer's instructions. Lipid peroxides (LPO) and protein carbonyls were measured using assay kits purchased from Cayman Chemical in accordance with the supplier's instructions. These measurements were made at 18 h post-stress. All cell-based assays were the average from at least three biological replicate experiments, each performed in quadruplicate.

Experimental Animals—All animal procedures were performed at Scripps (Jupiter, FL) accredited by the Association for Assessment and Accreditation of Laboratory Animal Care in accordance with protocols approved by the Institutional Animal Care and Use Committee of Scripps and the principles outlined in the National Institutes of Health Guide for the Care and Use of Laboratory Animals. Male Sprague-Dawley rats (Charles River Laboratories), 9–10 weeks old, were used in this study. The animals were housed in a controlled environment under a 12-h light/dark cycle and were allowed standard rat chow and water *ad libitum*.

6-Hydroxydopamine Lesion Surgery and Tat-Sab Treatment Procedure—Sprague-Dawley rats were randomly divided into three groups to receive saline + saline ($n = 5$), saline + 6-hydroxydopamine ($n = 9$), or Tat-Sab peptide + 6-hydroxydopamine ($n = 11$). Rats were anesthetized by intraperitoneal injection of a ketamine and xylazine mixture (70 and 8 mg/kg, respectively). Unilateral lesions of the right substantia nigra pars compacta were made by one 4- μl injection of 2 μg/μl 6-OHDA (Tocris Bioscience) in 0.1% ascorbate saline (0.9% sodium chloride) into the mid-forebrain bundle and three 2-μl injections of 2.1 μg/μl Tat-Sab peptide (NeoBioScience, MA) in saline. The final total dose of 6-OHDA was 8 μg, and the final dose of Tat-Sab was 42 μg/kg. The animals were placed in a Stoelting stereotaxic apparatus with the nose positioned 2.3 mm below the interaural line. Four burr holes were made to allow for injections at specific coordinates based on the atlas of Paxinos and Watson. The first, second, and third injections of either saline or Tat-Sab peptide were made at stereotaxic coordinates as follows: AP-5.5, ML −1.2 and DV −7.8; AP-4.8, ML −2.0 and DV −8.0; AP-6.2, ML −1.8 and DV −7.4, respectively. The fourth injection of either 6-OHDA or saline was made at AP-4.4, ML −1.2 and DV −7.8. The injections were made with a Stoelting Quintessential Stereotaxic Injector set at 1 μl/min with a 10-μl Hamilton syringe and 30-gauge 45° beveled tipped needle. The needle was left in place for 5 min post-injections to prevent backfilling along the injection tract. One week after the 6-OHDA lesions and Tat-Sab peptide injections, the efficacy of Tat-Sab peptide was determined by measuring rotational behavior following amphetamine administration.

Behavioral Testing—Rotational behavior was monitored with a Columbus Instrument Roto-Count-8 bowl cage system. Rats were attached to a harness and acclimated to the bowl cages for at least 10 min prior to amphetamine administration. Amphetamine (Sigma), 5 mg/kg, was given intraperitoneally 10 min prior to initiating measurement of rotation behavior. Both clockwise and counter-clockwise turning behavior was collected in seven 10-min intervals.

Immunohistochemistry—One hour following rotation testing, animals were sacrificed by an overdose of ketamine and xylazine followed by cardiac perfusion with 0.9% saline followed by 4% paraformaldehyde in a 0.1 M sodium phosphate buffer, pH 7.4. The brains were removed and further post-fixed in 4% paraformaldehyde at 4 °C for 1 day, followed by cryoprotection in 30% sucrose for 4 days. Brains were embedded and frozen in optimal cutting temperature compound and stored frozen at −80 °C until sectioning. Symmetrical 30-μm-thick sections were cut on a crytostat (Leica CM3050S) between approximately −4.4 and −6.6 mm bregma for ~73 sections. Every 3rd section (~21–24 sections) was processed for immunohistochemistry. Free-floating sections were pretreated in 0.3% H_2O_2 in tris-buffered saline (TBS) for 15 min and in blocking solution (4% bovine serum albumin (BSA) in TBS containing 0.1% Triton X-100) for 1 h at room temperature. In between steps, sections were washed three times for 15 min in TBS with 0.1% Triton X-100. For proper identification of the SNpc, all sections were incubated overnight at 4 °C with polyclonal rabbit anti-tyrosine hydroxylase (TH) (1:500; Abcam ab112) in 4% BSA in TBS containing 0.1% Triton X-100. Sections were then washed with TBS containing 0.1% Triton X-100 and incubated with anti-rabbit secondary antibody (1:500; Alexa Fluor 488) in 4% BSA in TBS containing 0.1% Triton X-100 for 2 h at room temperature in the dark. In between steps, sections were washed three times for 15 min in TBS. Sections were mounted on superfrost plus slides, and a drop of fluoroshield mounting medium with DAPI (1:4) was applied to each section. Slides were coverslipped, sealed with nail polish, and stored at 4 °C.

Stereological Counting of TH^+ Dopaminergic Cells—The total number of surviving TH^+ immunoreactive cells in the substantia nigra were estimated using unbiased stereology using the stereological software (Stereo Investigator 9, Microbrightfield Biosciences). Every other section of the immunostained sections was counted (or every 6th section between approximately −4.4 and −6.6 mm bregma) for a total of 10 sections for each animal. The optical fractionator probe consisted of a 50 × 50-μm counting frame with a height of 12 μm. The section thickness was estimated every dissector measurement and then averaged for each section.

Statistical Analysis—For behavioral rotation analysis, ipsilateral clockwise rotations were averaged for the group over each 10-min interval. Group differences were assessed at a significance level of $p < 0.05$ using a one-way ANOVA and Tukey's post hoc testing. TH^+ cell populations were estimated using number weighted section thickness and averaged for each group. In addition, the total area ($\mu m^{2)}$ of the SNpc analyzed for counting was averaged for each group. Group differences for TH^+ cell populations were assessed at a significance level of $p < 0.05$ using a one-way ANOVA and Tukey's post hoc testing.

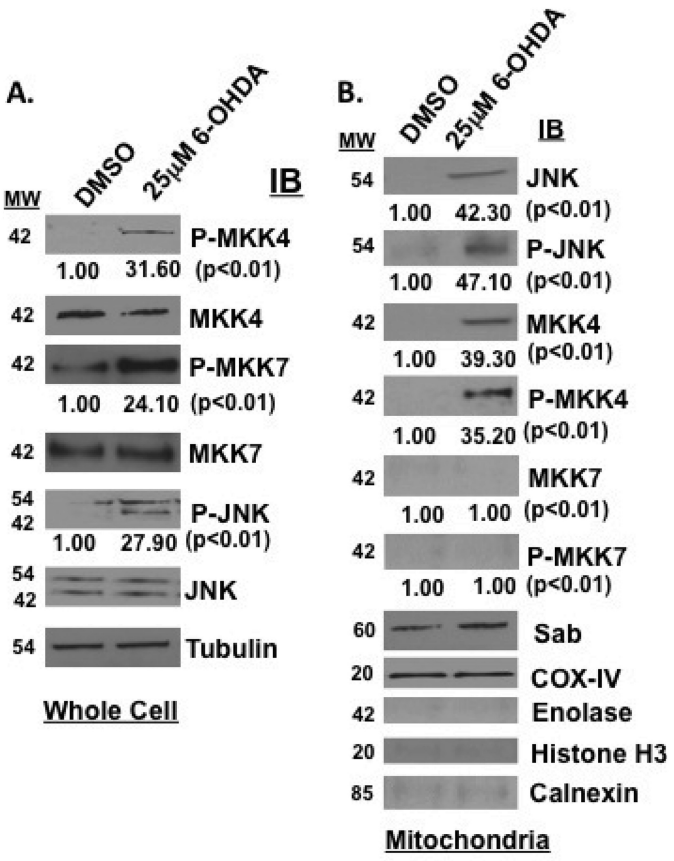

FIGURE 1. **6-OHDA activates the JNK pathway in SHSY5Y cells and induces JNK translocation to the mitochondria.** *A,* SHSY5Y cells were treated with 25 μM 6-OHDA for 4 h, and JNK signaling was evaluated by Western blot analysis. Proteins (30 μg) were resolved by SDS-PAGE, and antibodies for phospho-MKK4, MKK4, phospho-JNK, and JNK were used to detect proteins of interest in whole cell lysates. α-Tubulin was used as a loading control. *B,* mitochondrial isolations were prepared from SHSY5Y cells stressed with 25 μM 6-OHDA for 4 h. The mitochondria were monitored by Western analysis for JNK, phospho-JNK, MKK4, phospho-MKK4, MKK7, and phospho-MKK7. COX-IV served as the mitochondrial loading control. Enolase, histone H3, and calnexin blots are presented to demonstrate purity of mitochondrial preparations. *IB,* immunoblot.

RESULTS

To test the hypothesis that Tat-Sab$_{KIM1}$ could protect neuronal cells *in vitro* and *in vivo* by blocking JNK translocation to the mitochondria, we first had to establish that 6-OHDA activated the JNK pathway in cells and induced JNK mitochondrial translocation. To do this, we stressed SHSY5Y cells with 25 μM 6-OHDA for 4 h and monitored JNK pathway activation by Western analysis. Fig. 1 shows that the two JNK upstream activators, MKK4 and MKK7, as well as JNK itself were phosphorylated after 6-OHDA treatment as compared with DMSO treatment (Fig. 1*A*). In addition, mitochondrial isolation revealed that both MKK4 and JNK translocated to the mitochondria after 6-OHDA treatment and were not present before treatment. Moreover, both of these enzymes were phosphorylated (Fig. 1*B*). This is in contrast to Sab, which was present on the mitochondria at all times. COX-IV showed equal loading in all mitochondrial preparations. Enolase, histone H3, and calnexin blots were presented to demonstrate purity of mitochondrial preparations. These findings establish 6-OHDA as an activator and inducer of JNK to the mitochondrial outer membrane.

We next wanted to establish that this translocation caused oxidative stress, mitochondrial dysfunction, and neurotoxicity and that selective prevention of JNK translocation or inhibition of JNK catalytic activity could abrogate these abnormalities. To study oxidative stress, we monitored reduced glutathione (GSH) levels, LPO, and protein carbonylation (Fig. 2). For SHSY5Y cells treated with 25 μM 6-OHDA, there was a 25% decrease ($p < 0.05$) in GSSH levels compared with untreated cells. These GSSH levels were increased to near 90% of untreated control cells ($p < 0.05$) in the presence of 500 nM SR-3306, a potent selective JNK inhibitor shown to be efficacious in 6-OHDA lesions in rats (11). A similar increase in GSSH levels was seen when cells treated with 25 μM 6-OHDA had 10 μM Tat-Sab$_{KIM1}$ present or JNK siRNA or Sab siRNA present (Fig. 2*A*). 10 μM Tat-scramble peptide or control siRNA had no effect (Fig. 2*A*). For both LPO and protein carbonylation, treatment with 25 μM 6-OHDA caused an approximate 10-fold increase and 20-fold increase, respectively (Fig. 2, *B* and *C*), compared with untreated cells. Again, statistically significant protection for both of these measures was seen in the presence of either SR-3306, Tat-Sab$_{KIM1}$, or JNK siRNA or Sab siRNA compared with Tat-scramble, or control siRNA (Fig. 2, *B* and *C*).

To determine whether the 6-OHDA-induced and JNK-mediated ROS generation impacted mitochondrial function in SHSY5Y cells, we measured superoxide production with the mitochondria selective superoxide fluorophore MitoSOX Red. Treatment of cells with 25 μM 6-OHDA showed a 3-fold increase in MitoSOX fluorescence compared with untreated cells, with a statistically significant dose-dependent decrease in MitoSOX fluorescence in the presence of SR-3306. This same 2-fold decrease seen with 500 nM SR-3306 was also seen in the presence of 10 μM Tat-Sab$_{KIM1}$ but not Tat-Scramble peptide. siRNA for JNK or Sab also produced a statistically significant decrease in MitoSOX fluorescence compared with control siRNA (Fig. 3*A*). To assess mitochondrial function, we measured membrane potential utilizing JC-1 fluorescence, the OCR on a Seahorse analyzer, and ATP production. Again, treatment of cells with 25 μM 6-OHDA showed a 4.5-fold increase in JC-1 fluorescence that was reduced with a statistically significant dose-dependent effect in the presence of SR-3306 (Fig. 3*B*). This same 2.5-fold decrease seen with 500 nM SR-3306 was also seen in the presence of 10 μM Tat-Sab$_{KIM1}$ but not Tat-Scramble peptide as well as for siRNA against JNK or Sab (Fig. 3*B*). When the oxygen consumption rate and ATP production were measured, all four methods of JNK inhibition (SR-3306, Tat-Sab$_{KIM1}$, and siRNA for JNK or Sab) showed statistically significant improvements in these measures *versus* the controls (Fig. 3, *C* and *D*).

Although all of these measures showed that inhibition of JNK activity or JNK mitochondrial signaling had effects on oxidative stress and mitochondrial function, we also wanted to establish that inhibition of JNK mitochondrial translocation would also prevent 6-OHDA-induced cell death. First, we established that 5 μM Tat-Sab$_{KIM1}$ peptide but not 5 μM Tat-scramble peptide could block JNK translocation to the mitochondria (Fig. 4*A*).

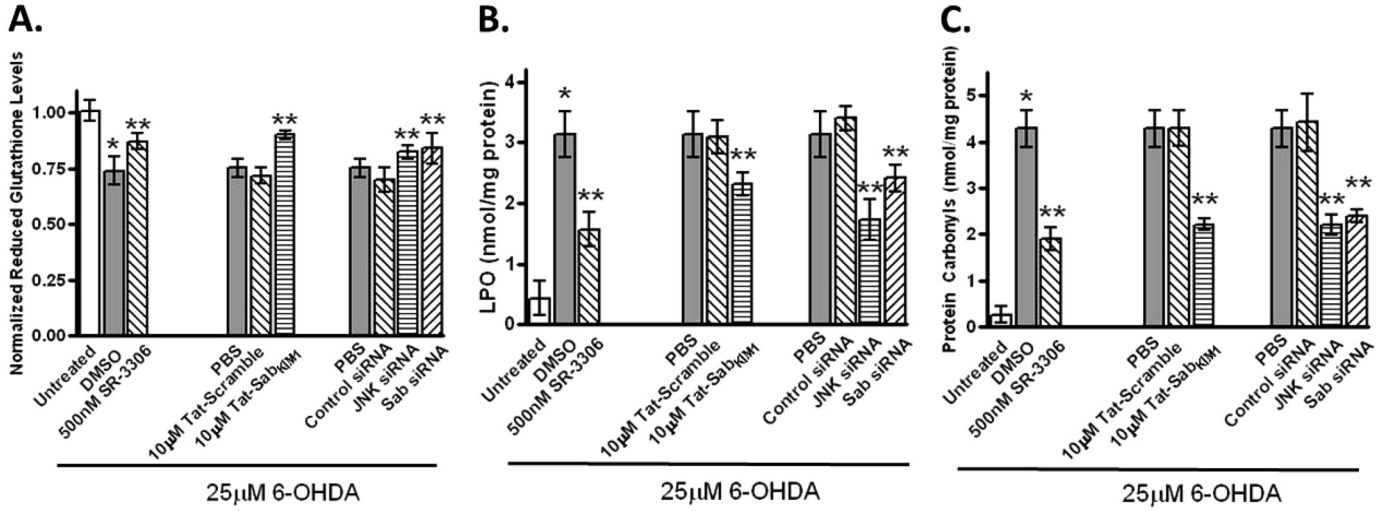

FIGURE 2. **Inhibition of mitochondrial JNK signaling and JNK activity prevents 6-OHDA-induced oxidative stress in SHSY5Y cells.** *A,* SHSY5Y cells were treated with 25 μM 6-OHDA for 18 h, and normalized reduced glutathione levels were measured in the presence or absence of 500 nM SR-3306, 10 μM Tat-Sab, or Tat-scramble peptide, JNK siRNA, Sab siRNA, or control siRNA. *B,* same as in *A* except LPO was measured. *C,* same as in *A* except protein carbonyls were measured. Significance ($p < 0.05$) between 6-OHDA-treated and -untreated groups is shown by * and between 500 nM SR-3306, 10 μM Tat-Sab or JNK siRNA, or Sab siRNA- and 6-OHDA-treated groups is given by **. The results are from at least three biological replicate experiments, each performed in quadruplicate.

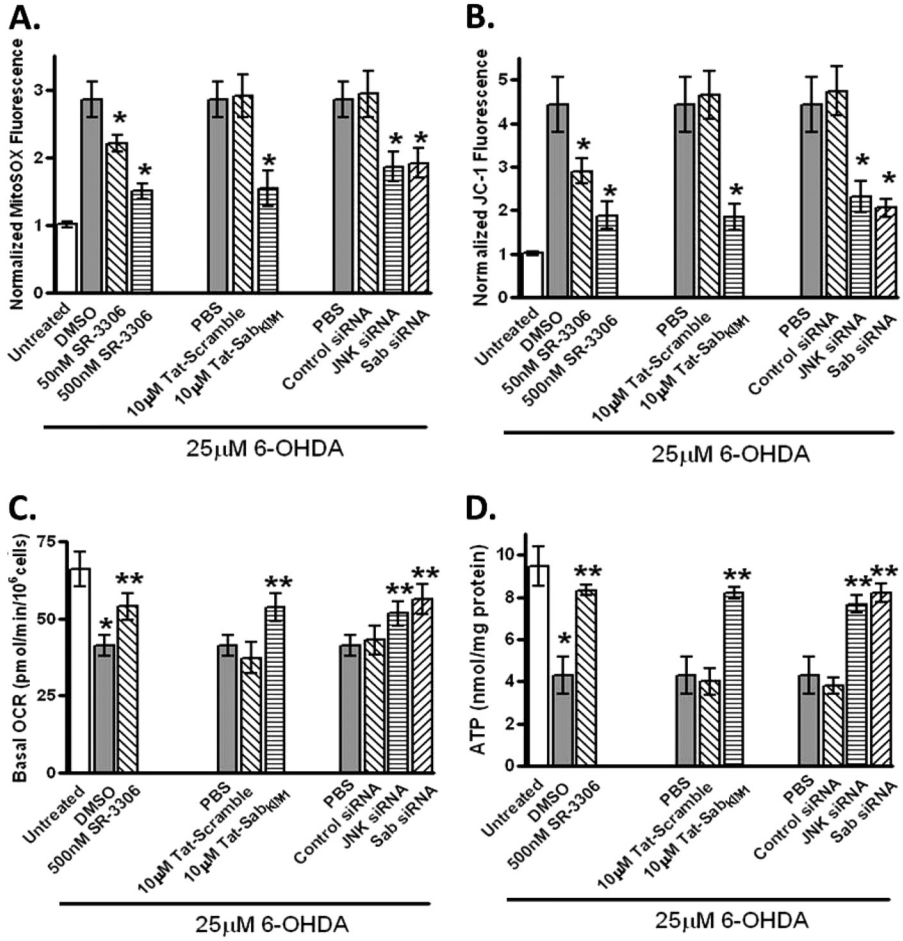

FIGURE 3. **Inhibition of mitochondrial JNK signaling and JNK activity prevents 6-OHDA-induced ROS generation, mitochondrial dysfunction, and changes in OCR and ATP levels in SHSY5Y cells.** *A,* SHSY5Y cells were treated with 25 μM 6-OHDA for 12 h, and mitochondrial ROS was measured by normalized Mitosox fluorescence in the presence or absence of 50 nM SR-3306, 500 nM SR-3306, 10 μM Tat-Sab or Tat-scramble peptide, JNK siRNA, Sab siRNA, or control siRNA. *B,* same as in *A* except mitochondrial membrane potential was measured by normalized JC-1 fluorescence after 18 h 6-OHDA stress. *C,* same as in *A* except OCR was measured in a Seahorse XF-96 analyzer after 12 h of 6-OHDA stress. *D,* same as in *A*; ATP levels were monitored by ATP determination kit (Invitrogen) after 12 h of 6-OHDA stress. Significance ($p < 0.05$) between 6-OHDA-treated groups and between 500 nM SR-3306, 10 μM Tat-Sab or JNK siRNA, or Sab siRNA and 6-OHDA-treated groups is shown by *. **, statistical significance ($p < 0.05$) between control treatment group and treated group. The results are from at least three biological replicate experiments, each performed in quadruplicate.

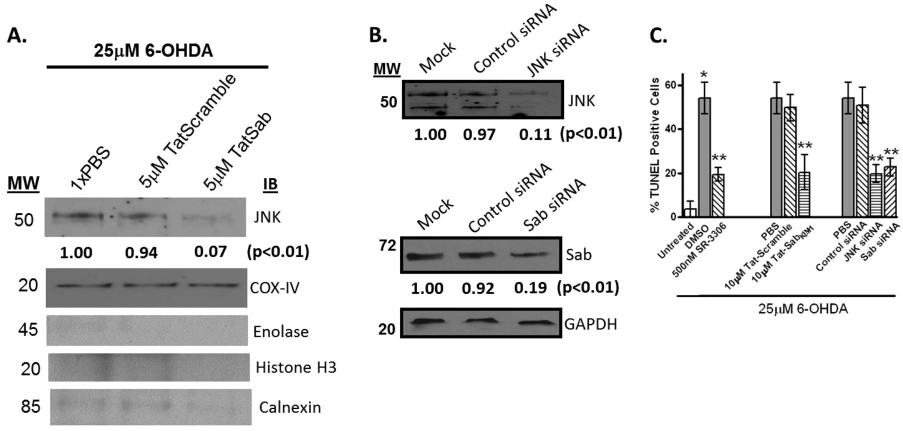

FIGURE 4. **Preventing JNK mitochondrial translocation and inhibiting JNK activity prevents 6-OHDA-induced cytotoxicity in SHSY5Y cells.** *A* and *B*, SHSY5Y cells were treated with 25 μM 6-OHDA for 4 h, and JNK translocation in the presence or absence of 5 μM Tat-Sab or Tat-scramble peptide, JNK siRNA or Sab siRNA, or control siRNA was evaluated by Western blot analysis. Proteins (30 μg) were resolved by SDS-PAGE, and antibodies for JNK were used to detect proteins of interest in whole cell lysates. COX-IV or GAPDH was used as a loading control. *C*, SHSY5Y cells were treated with 25 μM 6-OHDA for 4 h, and cell death was monitored after 24 h by TUNEL analysis in the presence or absence of 500 nM SR-3306, 10 μM Tat-Sab or Tat-scramble peptide, JNK siRNA, Sab siRNA, or control siRNA. Significance ($p < 0.05$) between 6-OHDA-treated and 500 nM SR-3306 or 10 μM Tat-Sab, or JNK siRNA, or Sab siRNA- and 6-OHDA-treated groups is given by **. *, statistical significance ($p < 0.05$) between untreated group and DMSO-treated group. The results are from at least three biological replicate experiments, each performed in quadruplicate. *IB*, immunoblot.

This finding was corroborated by knockdown of JNK or Sab by their respective siRNAs (Fig. 4, *B* and *C*). Having established knockdown of both JNK and Sab in the SHSY5Y cells and blocking of JNK translocation to the mitochondria, we next measured how these various inhibition mechanisms of JNK would affect cell death. Fig. 4*D* presents the % TUNEL-positive cells after 25 μM 6-OHDA treatment. The results showed that either inhibition of JNK activity by SR-3306, Tat-Sab_{KIM1}, JNK siRNA, or Sab siRNA all reduced the % TUNEL-positive cells by ~2.5-fold compared with 6-OHDA treatment and their control treatments (Fig. 4*D*). SR-3306 was also shown to inhibit c-Jun phosphorylation in SHSY5Y cells in a dose-dependent manner (supplemental Fig. 1).

To demonstrate that these findings were not specific to SHSY5Y cells, we also examined whether inhibition of mitochondrial JNK protects rat primary cortical neurons from generation of ROS, mitochondrial dysfunction, and cell death. Fig. 5 shows that either 500 nM SR-3306 or 10 μM Tat-Sab_{KIM1} reduced 6-OHDA-induced ROS generation by 2-fold (Fig. 5*A*). Similarly, mitochondrial dysfunction as measured by membrane potential showed strong protection from both 500 nM SR-3306 or 10 μM Tat-Sab_{KIM1} treatment (Fig. 5*B*). Finally, the % TUNEL-positive cells after 25 μM 6-OHDA treatment was reduced by 2.5-fold compared with 6-OHDA treatment and their control treatments (Fig. 5*C*). Collectively, these results suggest that inhibition of JNK activity or prevention of translocation to the mitochondrial membrane was protective against JNK-driven ROS production, membrane potential dissipation, and cell death both in a dopaminergic cell line and primary cortical neurons.

To test whether the protective effects seen *in vitro* could be manifested *in vivo*, we assessed whether Tat-Sab_{KIM1} could block dopaminergic cell loss in the SNpc of rats unilaterally lesioned with 6-OHDA and whether this manifested in behavioral protection. To do this, we stereotactically injected Tat-Sab_{KIM1} into three regions of the mid-forebrain bundle just prior to 6-OHDA treatment and allowed the lesion to develop over 7 days. Fig. 6*A* presents the unbiased stereological count for the number of TH^+ cells in the ipsilateral SNpc for three treatment groups as follows: saline/saline, saline/6-OHDA, and Tat-Sab_{KIM1}/6-OHDA. As expected, the 6-OHDA lesion reduced the number of TH^+ dopaminergic neurons by 3-fold compared with saline-treated animals ($p < 0.05$). Addition of 42 μg/ml Tat-Sab_{KIM1} increased the number of TH^+ cells in the ipsilateral side by ~2-fold compared with the 6-OHDA-lesioned animals that received vehicle ($p < 0.05$). (Fig. 6*A*). Fig. 6*B* shows that the total area measured in the SNpc following the 6-OHDA lesion was the same for all groups.

To establish whether the Tat-Sab_{KIM1}-protected nigrostriatal neurons were functional, we measured the rotational behavior of rats challenged with 5 mg/kg (intraperitoneally) of D-amphetamine 7 days after 6-OHDA lesions (Fig. 6*C*). In rats that received unilateral injections of 6-OHDA, D-amphetamine produced ~90 unilateral rotations in a 10-min interval, whereas saline-treated animals did not show a rotational bias. 6-OHDA-lesioned animals treated with 42 μg/ml Tat-Sab_{KIM1} showed an approximate 30% decrease in unilateral rotational behavior ($p < 0.05$) (Fig. 6*C*). Collectively, these results suggest that blocking JNK translocation to the mitochondrial membrane can exert neuroprotective effects that are manifested in behavioral improvement.

Finally, to ensure that Tat-Sab_{KIM1} had reasonable exposure in the SNpc, we utilized a TAMRA-labeled Tat-Sab_{KIM1} to visualize the distribution of the peptide in the SNpc. 24 h after 42 μg/kg TAMRA-Tat-Sab_{KIM1} was delivered as described, animals were sacrificed, and brain slices were taken to visualize the distribution in the SNpc. Fig. 7 shows that TAMRA-Tat-Sab_{KIM1} was widely distributed in this region of the brain. Moreover, steady-state analysis of TAMRA-Tat-Sab_{KIM1} revealed concentrations of the peptide in the brain of 95 μM at 0 h, 4 μM at 24 h, 1 μM at 3 days, and 750 nM at 7 days ensuring exposure levels at day 7 3-fold in excess of the biochemical IC_{50}.

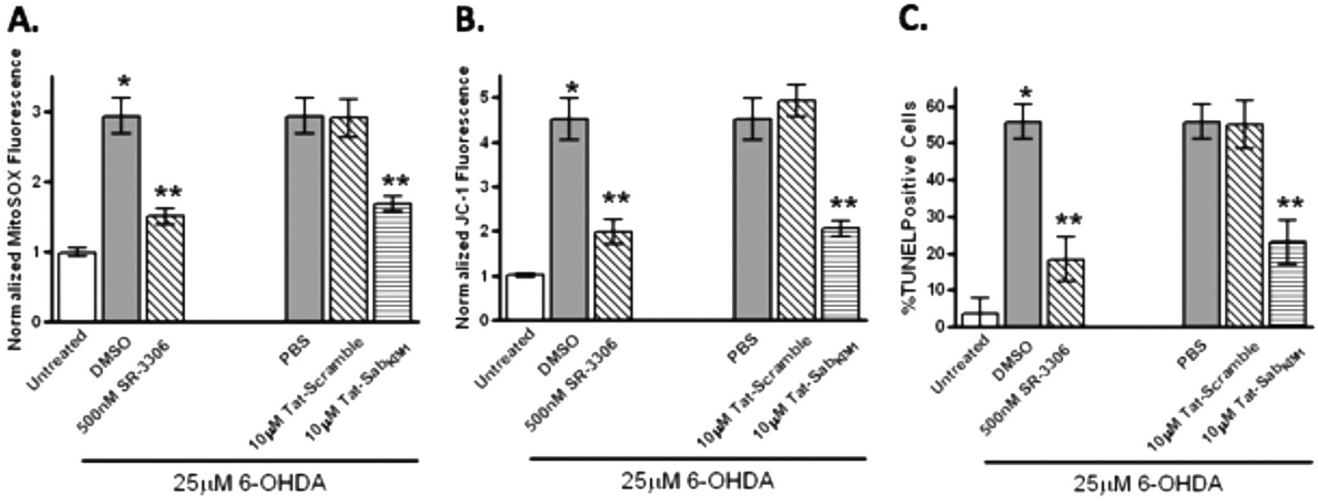

FIGURE 5. **Preventing JNK mitochondrial translocation and inhibiting JNK activity prevents 6-OHDA-induced ROS generation, mitochondrial membrane potential dissipation, and cytotoxicity in rat primary cortical neurons.** Rat primary cortical neurons were treated with 25 μM 6-OHDA for 12 h, and mitochondrial ROS was measured by normalized Mitosox fluorescence in the presence or absence of 500 nM SR-3306 or 10 μM Tat-Sab or Tat-scramble peptide. *B,* same as in *A* except mitochondrial membrane potential was measured by normalized JC-1 fluorescence at 18 h after 6-OHDA addition. *C,* same as in *A* except cell death was measured by TUNEL analysis at 24 h after 6-OHDA addition. Significance ($p < 0.05$) between 6-OHDA-treated and -untreated groups is given by * and between 500 nM SR-3306, 10 μM Tat-Sab, or JNK siRNA, or Sab siRNA- and 6-OHDA-treated groups is given by **. The results are from at least three biological replicate experiments, each performed in quadruplicate.

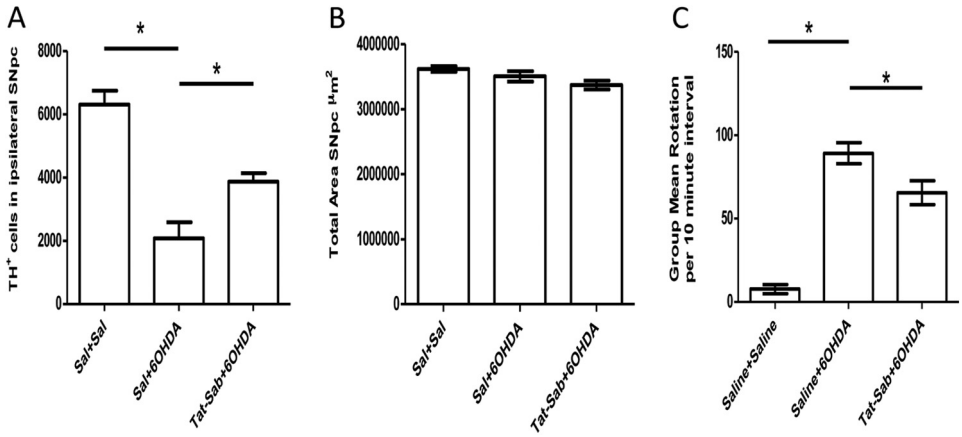

FIGURE 6. **Preventing JNK mitochondrial translocation *in vivo* protects dopaminergic neurons in the SNpc of rats lesioned with 6-OHDA and provides behavioral benefits.** *A,* unbiased stereological counts of TH-positive cells in the SNpc at 7 days after 6-OHDA treatment. Beginning at bregma −4.4, brains were sectioned at 30 μm for ~73 sections and ending at bregma −6.6. Three groups were analyzed as follows: saline/saline (*Sal*+*Sal*) ($n = 5$/group); 6-OHDA/saline ($n = 9$/group); and 6-OHDA/42 μg/kg Tat-Sab ($n = 11$/group). Eight μg of 6-OHDA was given by one injection into the medial forebrain bundle. For Tat-Sab-treated groups, Tat-Sab was given intracerebrally in the mid-forebrain bundle at the coordinates given under "Experimental Procedures." Data are expressed as the number of TH^+ neurons (±S.E.) surviving 7 days after the 6-OHDA treatment as detected by TH-immunohistochemistry (*, $p < 0.05$; established by one-way ANOVA also followed by Tukey's post hoc test). *B,* total area measured in the SNpc for the three groups. *C,* lesioned rats were given a D-amphetamine challenge (5 mg/kg, intraperitoneal) 10 min prior to measurement of rotation behavior. The rotation scores were collected in seven 10-min intervals with a computerized activity monitoring system (*, $p < 0.05$; established by one-way ANOVA also followed by Tukey's post hoc test).

DISCUSSION

One of the aims of this study was to determine the contribution of mitochondrial localized JNK to neurotoxin-driven neuronal cell death *in vitro* and *in vivo*. Based on observations we made in HeLa cells (6, 21), which showed that mitochondrial JNK was responsible for generating up to 80% of the ROS produced in a cell by an initial oxidative stress and contributed significantly to cell death, we reasoned the same may be true for neuronal cells. Indeed, we also showed that the mechanism by which JNK promoted ROS production and mitochondrial dysfunction was through complex I. We also wanted to extend those cell-based findings to an *in vivo* model of neurodegeneration by capitalizing on a cell-permeable selective peptide that enabled isolation of JNK mitochondrial contributions to cell death that were independent from its nuclear effects (6, 21).

Several conclusions can be drawn from our findings. First, it is clear that 6-OHDA activates the JNK pathway *in vitro* both in a human dopaminergic neuronal cell line and rat primary cortical neurons. These findings are consistent with those of Pan *et al.* (22) and Björklund and co-workers (23), where both groups showed that the JNK pathway was activated *in vivo* upon 6-OHDA lesions. Our findings extend these studies and show for the first time that JNK is translocated to the mitochondrial surface and that this translocation is mediated by the JNK-Sab interaction (Fig. 1). Furthermore, we show that this mitochondrial translocation is a critical component of oxidative stress,

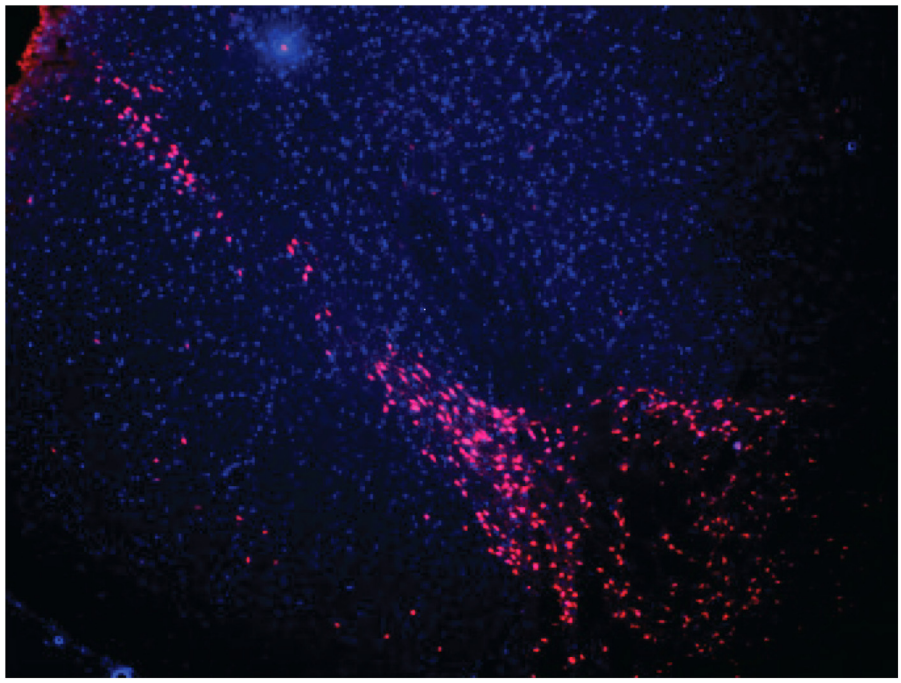

FIGURE 7. **Distribution of TAMRA-Tat-Sab in the SNpc.** A total dose of 42 μg/kg Tat-Sab was given as three injections (intracerebral ventricularly) as described under "Experimental Procedures." Animals were sacrificed 24 h after injection, and 30-μm sections were taken between bregma −4.4 and −6.6. DAPI was applied to each section, and TAMRA fluorescence was visualized on the Texas Red spectrum channel of an Olympus DP70 microscope.

mitochondrial dysfunction, and cell death (Figs. 2–5). Importantly, the near equal protection for mitochondrial function (Fig. 3*B*) against oxidative stress, OCR, and ATP levels by either 500 nM SR-3306 or 10 μM Tat-Sab in these cells suggests that inhibition of JNK mitochondrial signaling may be just as effective as inhibition of JNK activity in protecting the cell against mitochondrial dysfunction and cell death initiated by oxidative stress. The ramifications of this observation is that it provides the potential to develop inhibitors that selectively block the JNK-Sab interaction that would only block mitochondrial signaling leaving nuclear signaling intact.

We have previously shown by utilizing the same sets of reagents and *Jnk*$^{-/-}$ mouse embryonic fibroblasts that JNK increased superoxide production up to 80% in HeLa cells (6). The stressors and time course utilized in those studies were different from what was used in the studies reported here. However, it is likely that a similar phenomenon is happening in the neuronal cells as well. Initial oxidative stress is generated by the neurotoxin at complex I causing JNK to translocate to the mitochondria thereby amplifying ROS to cause mitochondrial dysfunction and cell death. Indeed, up to 85% of OCR and 90% of ATP levels may be related to JNK function.

A major finding for this study is the recapitulation of what is seen in the neuronal cells *in vivo*. namely protection of dopaminergic cell loss in the SNpc from 6-OHDA lesion with the treatment with Tat-Sab. Interestingly, the 2-fold protection in preserving DA neurons in the SNpc seen in this study was substantially less than the 8-fold protection we saw when we utilized SR-3306 (11). There are many possible explanations for this difference. First, the constant infusion of SR-3306 enabled steady-state levels of compound to be present in the brain for the entire 14-day period prior to sacrifice and counting of neurons. In this study, Tat-Sab was injected once, and peptide concentrations were assessed 24-h post dose (Fig. 7). Although the levels (750 nM) in the SNpc were significantly higher at that 24-h time point than the IC_{50} of Tat-Sab, it is almost certain that the peptide levels decreased over the course of lesion development, perhaps dropping to low levels, leaving not enough peptide to give full protection. Although this is purely speculation, the pharmacokinetics of peptide in the SNpc could easily and carefully be studied to prove or disprove this notion. Such a study was beyond the scope of this work as we merely wanted to see if the mechanism of blocking mitochondrial translocation would be neuroprotective *in vivo*.

A second potential explanation for the lower level protection could be that the dose of Tat-Sab was not optimized for maximal protection *in vivo*. *In vivo*, the pharmacokinetics may be such that the peptide gets hydrolyzed quickly, or diffuses from the site of action, or is actively transported away from the site of action. Many of these mechanisms are not operational *in vitro* and as such maximal efficacy is achieved. Therefore, a higher dose of Tat-Sab may suffice for maximal efficacy.

A third reason why the *in vivo* effects of SR-3306 were much better than Tat-Sab could be due to gene transcriptional effects that are occurring over the 7-day time course of this experiment. Because SR-3306 inhibits c-Jun phosphorylation that impacts gene transcription, the time course of those transcriptional events may be much more greatly impacted by the steady-state levels of SR-3306 blocking transcription for that time period thereby aiding in the efficacy by having these events turned off.

A fourth reason why the Tat-Sab peptide was less effective than SR-3306 at protecting dopaminergic neurons could be due to the delivery location of the peptide. Although our data show that injection at the coordinates we choose clearly delivered peptide to the SNpc at the 24-h time point, optimization of

this could potentially improve efficacy. Given our data, this possibility seems remote, but it is worth mentioning for completeness.

Finally, it should be noted that the lower protection seen by Tat-Sab peptide could indicate that inhibition of translocation to the mitochondrial surface is not as effective as global inhibition of JNK activity for protecting neurons *in vivo*. The data clearly show this in the 4-fold difference between the two studies, and if none of the other possibilities mentioned above are the explanation, then, all things considered equal, mitochondrial signaling may be less effective than overall JNK inhibition *in vivo*. We think this possibility is unlikely given the *in vitro* results, and that if all things were equal, protection from mitochondrial signaling would be very close to inhibition of global JNK signaling. Nevertheless, it is exciting to think that inhibition of JNK translocation to the mitochondria could be a novel therapeutic approach for neuroprotection. Designing inhibitors that strictly targeted the JNK-Sab interaction of course could easily test this. Our group is in the process of doing this now as we have solved the crystal structure of JNK with the Sab KIM1 peptide domain and have synthesized many bi-dentate inhibitors that bind in both the ATP pocket as well as the D-site.

In summary, this is the first demonstration on the molecular level that shows that blocking JNK mitochondrial signaling via inhibition of JNK interaction with Sab can be protective against neurodegeneration *in vivo*. In addition these results provide a mechanism by which JNK-driven mitochondrially generated ROS causes mitochondrial dysfunction in both human neuronal cells and primary neurons and that blocking the molecular interaction between JNK and Sab mitigates these dysfunctions manifesting in significantly reduced behavioral deficits, cell death, and oxidative stress *in vitro* and *in vivo*. These studies lay the foundation for designing mitochondrially specific JNK signaling inhibitors that may reduce any toxicities seen with JNK-dependent nuclear inhibition.

REFERENCES

1. Aoki, H., Kang, P. M., Hampe, J., Yoshimura, K., Noma, T., Matsuzaki, M., and Izumo, S. (2002) Direct activation of mitochondrial apoptosis machinery by c-Jun N-terminal kinase in adult cardiac myocytes. *J. Biol. Chem.* **277,** 10244–10250
2. Hanawa, N., Shinohara, M., Saberi, B., Gaarde, W. A., Han, D., and Kaplowitz, N. (2008) Role of JNK translocation to mitochondria leading to inhibition of mitochondria bioenergetics in acetaminophen-induced liver injury. *J. Biol. Chem.* **283,** 13565–13577
3. Zhao, Y., and Herdegen, T. (2009) Cerebral ischemia provokes a profound exchange of activated JNK isoforms in brain mitochondria. *Mol. Cell. Neurosci.* **41,** 186–195
4. Zhou, Q., Lam, P. Y., Han, D., and Cadenas, E. (2008) c-Jun N-terminal kinase regulates mitochondrial bioenergetics by modulating pyruvate dehydrogenase activity in primary cortical neurons. *J. Neurochem.* **104,** 325–335
5. Zhou, Q., Lam, P. Y., Han, D., and Cadenas, E. (2009) Activation of c-Jun N-terminal kinase and decline of mitochondrial pyruvate dehydrogenase activity during brain aging. *FEBS Lett.* **583,** 1132–1140
6. Chambers, J. W., and LoGrasso, P. V. (2011) Mitochondrial c-Jun N-terminal kinase (JNK) signaling initiates physiological changes resulting in amplification of reactive oxygen species generation. *J. Biol. Chem.* **286,** 16052–16062
7. Greenamyre, J. T., Sherer, T. B., Betarbet, R., and Panov, A. V. (2001) Complex I and Parkinson's disease. *IUBMB Life* **52,** 135–141
8. Moore, D. J., West, A. B., Dawson, V. L., and Dawson, T. M. (2005) Molecular pathophysiology of Parkinson's disease. *Annu. Rev. Neurosci.* **28,** 57–87
9. Schapira, A. H., Cooper, J. M., Dexter, D., Jenner, P., Clark, J. B., and Marsden, C. D. (1989) Mitochondrial complex I deficiency in Parkinson's disease. *Lancet* **1,** 1269
10. Chambers, J. W., Pachori, A., Howard, S., Ganno, M., Hansen, D., Jr., Kamenecka, T., Song, X., Duckett, D., Chen, W., Ling, Y. Y., Cherry, L., Cameron, M. D., Lin, L., Ruiz, C. H., and Lograsso, P. (2011) Small molecule c-Jun N-terminal kinase (JNK) inhibitors protect dopaminergic neurons in a model of Parkinson's disease. *ACS Chem. Neurosci.* **2,** 198–206
11. Crocker, C. E., Khan, S., Cameron, M. D., Robertson, H. A., Robertson, G. S., and Lograsso, P. (2011) JNK inhibition protects dopamine neurons and provides behavioral improvement in a rat 6-hydroxydopamine model of Parkinson's disease. *ACS Chem. Neurosci.* **2,** 207–212
12. Hunot, S., Vila, M., Teismann, P., Davis, R. J., Hirsch, E. C., Przedborski, S., Rakic, P., and Flavell, R. A. (2004) JNK-mediated induction of cyclooxygenase 2 is required for neurodegeneration in a mouse model of Parkinson's disease. *Proc. Natl. Acad. Sci. U.S.A.* **101,** 665–670
13. Xia, X. G., Harding, T., Weller, M., Bieneman, A., Uney, J. B., and Schulz, J. B. (2001) Gene transfer of the JNK interacting protein-1 protects dopaminergic neurons in the MPTP model of Parkinson's disease. *Proc. Natl. Acad. Sci. U.S.A.* **98,** 10433–10438
14. Wiltshire, C., Matsushita, M., Tsukada, S., Gillespie, D. A., and May, G. H. (2002) A new c-Jun N-terminal kinase (JNK)-interacting protein, Sab (SH3BP5), associates with mitochondria. *Biochem. J.* **367,** 577–585
15. Barr, R. K., Boehm, I., Attwood, P. V., Watt, P. M., and Bogoyevitch, M. A. (2004) The critical features and the mechanism of inhibition of a kinase interaction motif-based peptide inhibitor of JNK. *J. Biol. Chem.* **279,** 36327–36338
16. Barr, R. K., Kendrick, T. S., and Bogoyevitch, M. A. (2002) Identification of the critical features of a small peptide inhibitor of JNK activity. *J. Biol. Chem.* **277,** 10987–10997
17. Heo, Y. S., Kim, S. K., Seo, C. I., Kim, Y. K., Sung, B. J., Lee, H. S., Lee, J. I., Park, S. Y., Kim, J. H., Hwang, K. Y., Hyun, Y. L., Jeon, Y. H., Ro, S., Cho, J. M., Lee, T. G., and Yang, C. H. (2004) Structural basis for the selective inhibition of JNK1 by the scaffolding protein JIP1 and SP600125. *EMBO J.* **23,** 2185–2195
18. Ho, D. T., Bardwell, A. J., Grewal, S., Iverson, C., and Bardwell, L. (2006) Interacting JNK-docking sites in MKK7 promote binding and activation of JNK mitogen-activated protein kinases. *J. Biol. Chem.* **281,** 13169–13179
19. Borsello, T., Clarke, P. G., Hirt, L., Vercelli, A., Repici, M., Schorderet, D. F., Bogousslavsky, J., and Bonny, C. (2003) A peptide inhibitor of c-Jun N-terminal kinase protects against excitotoxicity and cerebral ischemia. *Nat. Med.* **9,** 1180–1186
20. Kaneto, H., Nakatani, Y., Miyatsuka, T., Kawamori, D., Matsuoka, T. A., Matsuhisa, M., Kajimoto, Y., Ichijo, H., Yamasaki, Y., and Hori, M. (2004) Possible novel therapy for diabetes with cell-permeable JNK-inhibitory peptide. *Nat. Med.* **10,** 1128–1132
21. Chambers, J. W., Cherry, L., Laughlin, J. D., Figuera-Losada, M., and Lograsso, P. V. (2011) Selective inhibition of mitochondrial JNK signaling achieved using peptide mimicry of the Sab kinase interacting motif-1 (KIM1). *ACS Chem. Biol.* **6,** 808–818
22. Pan, J., Zhao, Y. X., Wang, Z. Q., Jin, L., Sun, Z. K., and Chen, S. D. (2007) Expression of FasL and its interaction with Fas are mediated by c-Jun N-terminal kinase (JNK) pathway in 6-OHDA-induced rat model of Parkinson disease. *Neurosci. Lett.* **428,** 82–87
23. Vaudano, E., Rosenblad, C., and Björklund, A. (2001) Injury induced c-Jun expression and phosphorylation in the dopaminergic nigral neurons of the rat. Correlation with neuronal death and modulation by glial-cell-line-derived neurotrophic factor. *Eur. J. Neurosci.* **13,** 1–14